



**Acoustics'08  
Paris**  
June 29-July 4, 2008

[www.acoustics08-paris.org](http://www.acoustics08-paris.org)

## A hybrid SEA/image sources approach for the prediction of the insertion loss of enclosures

Franck Sgard<sup>a</sup>, Hugues Nelisse<sup>a</sup>, Nouredine Atalla<sup>b</sup>, Celse Kafui Amedin<sup>c</sup> and Rémy Oddo<sup>c</sup>

<sup>a</sup>IRSST, Service de la recherche, 505 Boulevard de Maisonneuve O, Montréal, QC, Canada H3A3C2

<sup>b</sup>Univ. de Sherbrooke, Mechanical Engineering Depart., 2500 Boulevard de l'Université, Sherbrooke, QC, Canada J1K 2R1

<sup>c</sup>GAUS, Université de Sherbrooke - 2500 Bd de l'Université, Sherbrooke, QC, Canada J1K2R1  
frasga@irsst.qc.ca

Enclosures are a classical solution to reduce the sound exposure of workers to the noise radiated by machinery. Their acoustic design can be achieved with the help of predictive tools based on simple analytical tools or sophisticated numerical deterministic models. However, there is no simple and fast tool allowing to account for the complexity of the enclosure configuration, capable of better simulating the non-diffuse nature of the field inside the enclosure and covering the typical frequency range [100Hz; 5000Hz]. This paper presents the development of such a tool for the prediction of the acoustic performance of enclosures. It is based on a hybrid model: the statistical energy analysis (SEA) for the sound transmission across the various elements of the enclosure and the method of image sources for the sound field inside the enclosure. The approach is validated by comparing calculation and experimental results carried out in a semi-anechoic room on rectangular and L-shape enclosures for several inner source locations. The effect of an opening is also investigated. The comparisons between the models and the experimental results show a good agreement for most of the tested configurations.

## 1 Introduction

Large enclosures or cabin enclosures are a common noise control solution to reduce the airborne sound radiated by a noisy machine. They consist of a box surrounding the noise source which is made up of an assembly of multilayered structures (metal or wood skin which can be stiffened, a sound absorbing material (e.g mineral wool) and a perforated metal plate or an impervious screen). The acoustic performance of an enclosure is usually assessed by its insertion loss which is the difference between the sound power of the source in free field and the sound power transmitted by the enclosure surrounding it. The insertion loss depends on multiple factors: sound transmission loss of each component, absorbing materials inside the enclosure, presence of leaks and apertures, coupling between the machine, the ground and the enclosure walls, position and extent of the machine.

Extensive work has been done in the past on acoustic enclosures. At high frequencies, energy based methods are commonly utilized. Simplified models based on the calculation of the sound power radiated from the enclosure through the various non resonant transmission paths (structural, leaks etc.) have been developed to design enclosures [1-3]. Comparisons between the theory and experimental results indicate that insertion loss trends are correctly captured especially in the case of sealed enclosures made up of single walls with acoustical treatment but not for double walls [2]. Other energy based techniques like ray tracing, mixed BEM-ray tracing and energy flow method allow for the calculation of the sound transmission through flexible panels and can be used to predict the insertion loss of machinery enclosures. Ray-tracing method is classically used in architectural acoustics where only the room internal sound field is needed. Walls are then assumed not to vibrate. Barbry [4] is currently extending the ray-tracing technique by considering the rays transmitted through enclosure panels in order to calculate its sound insertion loss. Jean [5] combined the ray tracing technique to assess the Green's function and the BEM to predict the internal and external sound field in cavities with flexible surfaces. Le-Bot [6] and Cotoni et al [7] developed an integral energy approach to predict the sound field inside an enclosure and for fluid-structure interaction problems respectively. Several authors also proposed Statistical Energy Analysis approaches for assessing the insertion loss of enclosures for internal sound excitation [8, 9] or placed into an external diffuse field [10-12]. Ver [8], Cole et al [11] and Ming and Pan [12] included both resonant and non

resonant transmission paths in their analysis whereas Lyon [10], Eichler [13] and Oldham [9] only considered resonant transmission. In the most recent work, Ming and Pan [12] proposed actually two different SEA based models accounting for the structural coupling between the walls and depending on the importance of the cavity modal density. The authors show that comparisons between the models and the experiments are encouraging. They insist on the fact that acoustical materials increase the damping in the cavity but also modify the non resonant transmission through enclosure panels. However, the materials are supposed to have only a mass effect and no rigorous model of their effect on the non-resonant transmission has been considered. Note that the discrepancies between the simulation and the experimental results for the treated enclosure could also be explained by the fact that the internal sound field is not really diffuse. In a real enclosure, the classical diffuse field assumption for the sound field is indeed likely not to hold because of the sound absorbing treatment. In addition SEA does not account for the source location inside the enclosure which may modify the insertion loss of the system especially in the presence of apertures and for complex shaped enclosures. This work is part of a research project aiming at developing simple and efficient design tools for machinery enclosures. The model is based on a mixed SEA-image sources approach which allows one to alleviate some of the previous limitations associated to classical SEA. The SEA framework is used here to solve the general problem. The image sources approach is used to calculate the internal sound field which is then considered as an equivalent source of pressure in the SEA equations. There are several originalities in the present approach (i) benefit of the latest model developments for the vibroacoustic behavior of multilayered acoustical materials based on transfer matrix approach (eg perforated plate+porous material) (ii) acoustical materials are accounted for through both their acoustic absorption and insertion loss using the transfer matrix approach, (iii) a new model for diffused field sound transmission loss through apertures is considered, (iv) a low frequency correction to account for the non diffuseness of the interior sound field is implemented [14] (v) a simplified model based on SEA, corrected with the direct field to represent the interior sound field, is developed (vi) the image sources method is combined with SEA to improve the quality of results in the whole frequency range. The models are validated using an experimental set-up consisting of two types of enclosures (parallelepipedic and L-shaped geometries) placed in a semi-anechoic room. Insertion losses are measured using the intensity scan method and compared to prediction results. In the following, the theory behind the model is

presented followed by a description of the experimental set-up and the validation results.

## 2 Theory

The enclosure is made up of an assembly of flexible homogeneous panels of uniform thickness treated with sound absorbing treatments. Panels can comprise apertures (leaks or openings). Inside the enclosure, a sound source whose dimensions are small compared to the acoustic wavelength generates an internal sound pressure field which makes the walls vibrate and radiate noise outside the enclosure. Both box and L-shaped geometries are considered. They are placed in a semi-anechoic room. Figure 1 displays the configuration of the L-shaped enclosure.

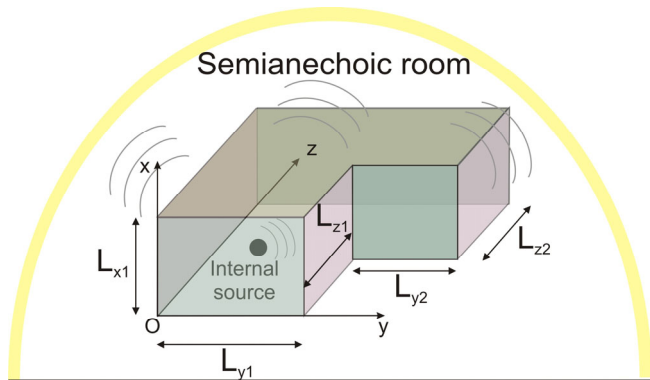


Fig.1 L-shaped enclosure surrounding a noise source and radiating inside a semi anechoic room

In the following, the enclosure panels are assumed to vibrate in bending motion, to have a sufficiently large modal density and to be mechanically uncoupled. Note that the tool which has been developed in the scope of this project is general and can also account for mechanical coupling. The enclosed air cavity is also considered to have a sufficient modal density.

### 2.1 SEA model

SEA gives a general framework to solve the global problem. The matrix form makes it easy for the enclosure to be much more complicated geometrically (as many subsystems (panels, apertures) as desired) and physically (eg additional structural couplings between panels, structure borne excitation possible, etc.).

Each panel together with the enclosed air volume and the external space surrounding the enclosure are treated as separate SEA subsystems. The external space is modelled as a very large absorbing cavity in order to simulate sound radiation in open space and it allows for the power flow from the external space to each panels to be negligible.

SEA equations consist in writing power flow balances for all the subsystems. They are classical and read:

$$\omega[A]\{E\} = \{\Pi\} \quad (1)$$

Where  $\omega$  is the circular frequency,  $\{E\}$  is the vector of total energies stored in each subsystem,  $\{\Pi\}$  is the vector

of injected powers in each subsystem and  $[A]$  is the loss factor matrix. All quantities are averaged over both space and frequency.

One has  $A_{ii} = \eta_{ii} + \sum_{\substack{j=1 \\ j \neq i}}^N \eta_{ji}$  and  $A_{ij} = -\eta_{ji}$  if  $j \neq i$  where  $\eta_{ij}$

denotes the coupling loss factor between subsystem  $i$  and subsystem  $j$ . The reciprocity equation  $n_i \eta_{ij} = n_j \eta_{ji}$  where  $n_i$  is the modal density of subsystem  $i$ , can be exploited to assess the loss factor from subsystem  $i$  to subsystem  $j$ . The modal densities of each subsystem are classical and can be found in [15].

### 2.2 Damping loss factors

The damping loss factor of the panels has to be measured by classical techniques. The damping loss factor of the cavities is given by:

$$\eta_{ii} = \frac{c_0 S_i \bar{\alpha}_i}{4 \omega V_i} \quad (2)$$

Where  $V_i$  and  $S_i$  are respectively the volume and the area of the surface enclosing cavity  $i$ ,  $\bar{\alpha}_i$  is the average diffuse field sound absorption coefficient of cavity  $i$ .

### 2.3 Coupling loss factors

The resonant coupling loss factor between a panel  $i$  and a cavity  $j$  is calculated from:

$$\eta_{ij}^{res} = \frac{\rho_0 c_0 \sigma_p}{\rho_s \omega} \left( \frac{S_{ray}}{S_p} \right) \quad (3)$$

where  $\sigma_p$  is the panel radiation efficiency,  $\rho_0$  and  $c_0$  are the air density and sound speed respectively,  $\rho_s$  is the panel surface mass density,  $S_{ray}$  is the radiating surface,  $S_p$  is the plate area.  $\sigma_p$  can be calculated using Leppington's formulas [16] which is valid for a baffled simply supported panel. At low frequencies  $\sigma_p$  can be corrected [15] to take into account the fact that the panel is not embedded into a plane rigid baffle and that the boundary conditions may be different from simply supported (say eg clamped) and comprise stiffeners. In reality indeed, the boundary conditions of the panel are somewhere in between simply supported and clamped. In addition, the panel radiates into a space delimited by plates at right angle ( $90^\circ$  on the source side and  $270^\circ$  on the external side).

The non resonant coupling loss factor between a cavity  $i$  and a cavity  $j$  is calculated from

$$\eta_{ij}^{nres} = \frac{c_0 S_{coup} \tau_p}{4 \omega V_i} \quad (4)$$

where  $\tau_p$  is the diffuse field sound transmission factor of the infinite panel separating the two cavities and  $S_{coup}$  is the coupling area. It is usual to keep only the mass law behaviour of the panel. Here the transmission loss is

calculated using a transfer matrix approach (Nova ©) and both stiffness and damping parts which are important around and above the critical frequency are retained.

For a panel treated with an acoustical material characterized by its insertion loss  $IL$  (defined as the difference between the transmission loss with and without treatment), both resonant and non resonant paths must be corrected. For the non resonant path, the transmission factor referred to in (4) has to be modified according to:

$$\tau_{p+trat} = \tau_p \times 10^{-\frac{IL}{10}} \quad (5)$$

and for the resonant path, the panel radiation efficiency  $\sigma_p$  appearing in eq(3) becomes

$$\sigma_{p+trat} = \sigma_p \times 10^{-\frac{IL}{10}} \quad (6)$$

It is worth mentioning that the same insertion loss is used to evaluate the correction for both the resonant and non resonant part. It has been shown that this is a reasonable assumption [17]. Here, the insertion loss is calculated using Nova (© Mecanum Inc). The damping added by the material can also be assessed using this software. Note however that the damping of the bare panel in place has to be measured in order to quantify a meaningful value of the added damping. In the present paper, this effect has not been into account to calculate the resonant part.

The leaks or openings are modeled as non resonant paths. The coupling loss factor is given by Eq.(4) where  $S_{coup}$  is the aperture area and  $S_{coup}$  corresponds now to the transmission loss is predicted using the modal approach proposed in [18].

## 2.4 Modeling of the internal sound field

In the current approach, the interior sound field is calculated using the image sources method instead of using a SEA based equation. The calculated average mean square sound pressure is then used to obtain the average energy in the cavity which is used as a constraint in Eq.(1). The system can then be solved and the enclosure insertion loss calculated as the difference between the sound power level radiated by the sound source  $L_{w0}$  and the enclosure  $L_w$  respectively:

$$IL = L_{w0} - L_w \quad (7)$$

In the image sources method, the sound pressure field at a point M in the enclosure due to a source located at a point  $M_0$  is considered as an infinite sum of the contributions of acoustic fields created by virtual sources which are images at multiple orders of the real source through the different walls of the enclosure together with the direct acoustic field. In practice the sound field at a point M can be approached by a finite number of contributing sources. The algorithm consists in generating the multiple virtual sources and discarding those which do not pass certain geometric tests (validity, visibility) as described by Borish [19].

Assuming a temporal dependency  $e^{j\omega t}$ , the coherent sound pressure at a given point in the enclosure writes:

$$\hat{p}(M) = \frac{e^{-jk_0 r}}{4\pi r} + \sum_{i=1}^N \hat{\mathfrak{R}}_i \frac{e^{-jk_0 r_i}}{4\pi r_i} \quad (8)$$

- R is the distance between the receiver M and the source  $M_0$
- N is the number of contributing sources for a specified order
- $r_i$  is the distance between the receiver M and the image source of order  $N_i$
- $\hat{\mathfrak{R}}_i$  is the global reflection coefficient corresponding to the walls which are intersected by the segment linking the source number i of order  $N_i$  and receiver M. If a specular reflection model is assumed, this coefficient is

equal to  $\hat{\mathfrak{R}}_i = \prod_{j=1}^{N_i} \hat{\mathfrak{R}}_{ij}(\theta_{ij})$  where  $\hat{\mathfrak{R}}_{ij}(\theta_{ij})$  is the

reflection coefficient of the wall which depends in principle on the incidence angle between the vector linking the image source i and receiver M and the normal to the intersected walls.

To get the complex valued reflection coefficient at oblique incidence  $\hat{\mathfrak{R}}_{ij}(\theta_{ij})$ , spherical wave or plane wave reflection models can be considered depending on the desired accuracy. The associated coefficients can be obtained from the normal incidence surface impedance of the sound absorbing treatments (if available) assuming a locally reacting behaviour. Assuming that  $\hat{\mathfrak{R}}_{ij}(\theta_{ij})$  is a real number, it can also be derived from the normal incidence sound absorption coefficient (if available), the statistical sound absorption coefficient (if available) or the Sabine sound absorption coefficient which is usually the data provided by the manufacturer. The reflection coefficient does not depend then on the incidence angle anymore. If the incidence angle is to be accounted for in the calculation, the locally reacting assumption can be used again to derive an associated normal surface impedance to the aforementioned absorption coefficients which can then be substituted to recalculate an oblique incidence plane wave or spherical wave reflection coefficient.

If incoherent sound pressure is desired Eq(8) can be rewritten as:

$$|\hat{p}(M)|^2 \approx \frac{1}{16\pi^2 r^2} + \sum_{i=1}^N |\hat{\mathfrak{R}}_i|^2 \frac{1}{16\pi^2 r_i^2} \quad (9)$$

One can classically use  $|\hat{\mathfrak{R}}_i|^2 = \prod_{j=1}^{N_i} |\hat{\mathfrak{R}}_{ij}|^2 = \prod_{j=1}^{N_i} (1 - \alpha_{ij})$ .

The equation can be corrected by adding a residual term  $R_N$  to take into account the contribution of the remaining image sources. This term is obtained by assuming that the residual field is reverberant and is equal to the power absorbed by the room after the Nth reflection [20]. The correction factor simply reads:

$$R_N = \frac{4(1 - \bar{\alpha})^{N+1}}{S\bar{\alpha}} \quad (10)$$

### 3 Experimental set-up

A box-shaped together with a L-shaped enclosures have been manufactured in order to investigate the effects on the insertion loss of the acoustical treatment, of the presence of an opening and of the source location (see fig.2). The walls of the enclosure consisted either of 1.16mm thick metal sheets or 1.61cm thick presswood panels. The sound treatment was made up of 7cm thick rockwool (Roxul) covered with a 1mm thick steel perforated plate. The panels were bolted on tubular steel frames filled with urethane foam. Duct seal was used to avoid acoustic leaks especially around the junctions between the panels and the door and the panels and the floor. To access the interior of the enclosure, a sandwich door consisting of two 1mm thick steel plates with a core of rockwool was manufactured.



Fig.2 Box-shaped and L-Shaped enclosures

	Material	Shape	Acoustic treatment	Source location [1 2 3]	Opening
1	Steel	Box	✓	○	
2	Steel	Box	✓	○	
3	Steel	Box	✓	○	✓
4	Steel	Box	✓	○	✓
5	Steel	L	✓	●	✓
6	Steel	L	✓	○	✓
7	Steel	L	✓	○	✓
8	Steel	L	✓	●	
9	Steel	L	✓	○	
10	Steel	L	✓	○	
11	Wood	L	✓	●	
12	Wood	L	✓	○	
13	Wood	L	✓	○	
14	Wood	L	✓	●	✓
15	Wood	L	✓	○	✓
16	Wood	L	✓	○	✓
17	Wood	Box	✓	○	✓
18	Wood	Box	✓	○	✓
19	Wood	Box	✓	○	
20	Wood	Box	✓	○	
21	Wood	Box	✓	○	
22	Wood	Box	✓	○	
23	Steel	Box	✓	○	
24	Steel	Box	✓	○	
25	Steel	Box	✓	○	✓
26	Steel	Box	✓	○	✓

Table 1 List of tested configurations

Table 1 displays the list of the tested configurations. The enclosures external dimensions are provided in table 2. The sound field inside the enclosure was created by both a B&K omnidirectional sound source and a compression chamber in order to deliver sufficient power in the frequency band of interest [80-6300Hz]. The sound powers of the two sources have been measured in a semianechoic room using a moving semicircular antenna of microphones located in the far field. Internal microphones have been positioned inside the enclosures to spatially sample the sound field (8 in the rectangular box and 11 in the L-shaped box). An additional microphone close to the sources was also used as a reference. The acoustic power radiated by the enclosure was measured by intensity scanning. A sound intensity probe was used to scan all the faces one by one. In the configurations where the opening was present, a special attention was paid when scanning the opening. Preliminary

intensity measurements allowed one to check the presence of leaks and ensure that the enclosure was correctly sealed.

	Lx [m]	Ly1 [m]	Lz1 [m]	Ly2 [m]	Lz2 [m]
Box	1.52	1.3	2.0	-	-
L-shape	1.52	1.3	1.0	1.0	1.0

Table 2 Dimensions of the enclosures

### 4 Results

In the calculation, the field incidence sound absorption coefficient is calculated using a transfer matrix approach (Nova © Mecanum Inc) and used in the equations. In the image sources technique, a coherent summation based a real reflection coefficient independent on the incidence angle has been used.

As a first example, Fig.3 shows the comparison between the measurements and the calculations for configuration number 1 (see tab.1). In the legend, “reverberant only” corresponds to a pure SEA model (diffuse reverberant field inside the enclosure), “reverb+direct” corresponds to a simplified model based on one SEA cavity corrected with the direct field to represent the interior sound field. Note the latter model has shown to be appropriate for a convex-shaped enclosure and a simple point source but should fail for more complicated geometries like L-shaped and extended sources. It is seen that both the mixed image sources and the simplified model accounting for the direct field are in a very good agreement with the measurements. The coherent image sources technique improves the result quality at low frequencies except for the first third octave frequency bands. Despite that the calculation for the interior sound field only accounts for the reverberant part, it can be observed that the pure SEA model is within 5dB from the experimental data and predicts the trend correctly.

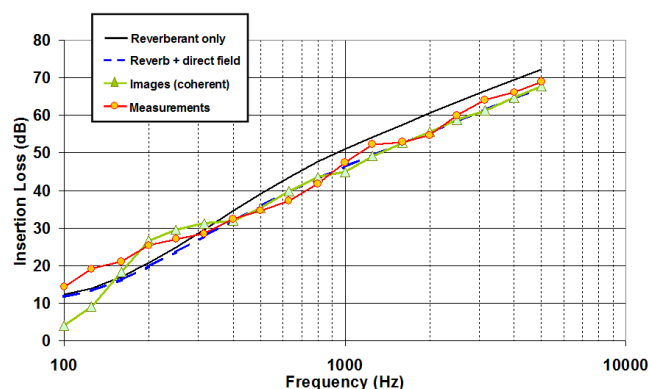


Fig.3 Comparisons between experimental data, SEA model, simplified SEA+direct model and coherent image sources model of the interior sound field in a box-shaped treated enclosure

As a second example, Fig.4 shows the comparison between the measurements and the calculations for configurations number 3 and 4 (see tab.1) which correspond to a treated box with an opening of 200mmx400mm and two different

source locations. In the "reverb+direct" calculations, the interior cavity has been split into two subcavities to account for the source position. Fig.4 indicates that the two models capture very well the effect of the source position on the insertion loss. As expected, when the source is close to the opening the insertion loss is decreased in particular at high frequencies. Again the image sources method allows one to reproduce satisfactorily the acoustic behavior of the enclosure at low frequencies.

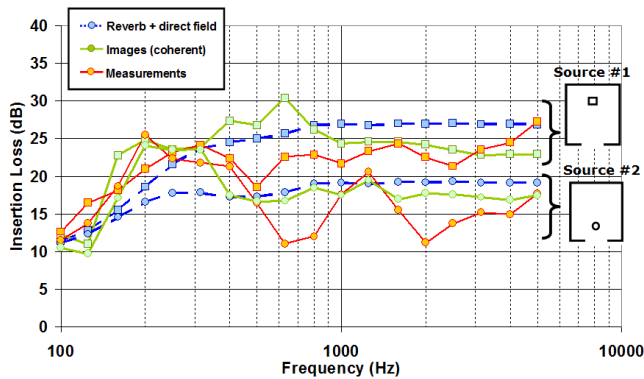


Fig.4 Comparisons between experimental data, simplified SEA+direct model and coherent image sources model of the interior sound field in a box-shaped treated enclosure with an opening and two source positions

## 5 Conclusion

This paper presented a general model to predict the sound insertion loss of large enclosures. It is based on a hybrid method relying on the statistical energy analysis (SEA) for the sound transmission across the various elements of the enclosure and the method of image sources for the sound field inside the enclosure. A simplified model based on SEA corrected with the direct field to represent the interior sound field has also been developed. Both approaches have been validated by comparing calculation and experimental results on rectangular and L-shaped enclosures for several interior source locations. The effect of an opening has also been investigated. The comparisons between the models and the experimental results showed a good agreement for most of the tested configurations. The coherent image sources model improves the prediction at low frequencies compared to the simplified model.

## Acknowledgments

The authors want to thank Institut Robert Sauvé en Santé et Sécurité du Travail (IRSST), Ecole Nationale des Travaux Publics de l'Etat (ENTPE) and Institut National en Recherche et Sécurité (INRS) for their financial support.

## References

- [1] CETIM, "Insonorisation des machines par encoffrement. Recueil de conférences". Senlis: Publications CETIM. 149 (1995)
- [2] N. Trompette, T. Loyau, and G. Lovat, "Encoffrements de machine - Aide à la conception : règles de base et mise en oeuvre expérimentale", *Cahiers de notes documentaires INRS - Hygiène et sécurité du travail* 182. 49-72 (2001)
- [3] E. O'Keefe. "A computer simulation for determining far-field noise levels radiated from a noise source within a rectangular enclosure". in *Inter-Noise*. Miami, USA. (1980)
- [4] J.L. Barbry and N. Trompette, "Amélioration des calculs prévisionnels des performances acoustiques de parois et d'encoffrements de machines", département Ingénierie des équipements de travail de l'INRS. (2007)
- [5] P. Jean, "Coupling geometrical and integral methods for indoor and outdoor sound propagation - validation examples", *Acta Acustica*. 87. 236-246 (2001)
- [6] A. Le Bot and A. Bocquillet, "Comparison of an integral equation on energy and the ray-tracing technique in room acoustics", *Journal of the Acoustical Society of America*. 108(4). 1732-1740 (2000)
- [7] V. Cotoni, A. Le Bot, and L. Jezequel, "Sound transmission through a plate by an energy flow approach", *Acta Acustica united with Acustica*. 88. 827-836 (2002)
- [8] I.L. Ver. "Reduction of noise by acoustic enclosures". in *Proc of ASME Design Engineering Technical Conference*. Cincinnati. (1973)
- [9] D.J. Oldham and S.N. Hillarby, "The acoustical performance of small close fitting enclosures, part 1: theoretical models", *Journal of Sound and Vibration*. 150(2). 261-281 (1991)
- [10] R.H. Lyon, "Noise reduction of rectangular enclosures with one flexible wall", *Journal of the Acoustical Society of America*. 35(11). 1791-1797 (1963)
- [11] V. Cole, M.J. Crocker, and P.K. Raju, "Theoretical and experimental studies of the noise reduction of an idealized cabin enclosure", *Noise Control Eng. J.* 20(3). 122-132 (1983)
- [12] R. Ming and J. Pan, "Insertion loss of an acoustic enclosure", *Journal of the Acoustical Society of America*. 116(6). 3453-3459 (2004)
- [13] E. Eichler, "Thermal circuit approach to vibrations in coupled systems and the noise reduction of a rectangular box", *Journal of the Acoustical Society of America*. 37(6). 995-1007 (1965)
- [14] P. Shorter, "Rigid walled cavities and SEA - Technical Memorandum", PJS-0117-01. (2001)
- [15] R. Craik, "Sound transmission through buildings using SEA". Gower (1996)
- [16] F.G. Leppington, E.G. Broadbent, and K.H. Heron, "The acoustic radiation efficiency of rectangular panels", *Proceedings of the Royal Society of London. Series A, Mathematical and Physical Sciences*. 382(1783). 245-271 (1982)
- [17] H. Nélisse, T. Onsay, and N. Atalla. "Structure-borne insertion loss of sound package components". in *SAE Meeting*. Detroit, MI, USA. (2003)
- [18] F. Sgard, H. Nélisse, and N. Atalla, "On the modeling of diffuse field sound transmission loss of finite thickness apertures", *Journal of the Acoustical Society of America*. 122(1). 302-313 (2007)
- [19] J. Borish, "Extension of the image model to arbitrary polyhedra", *Journal of the Acoustical Society of America*. 75(6). 1827-1836 (1984)
- [20] A. L'Espérance, "Logiciel d'analyse et de gestion du bruit OUIE 2000 - développement et intégration d'un modèle d'acoustique prévisionnelle", IRSST, R-271. (2001)